

Loading and Response of Offshore Wind Turbine Support Structures: Prediction with Comparison to Measured Data

Authors

K. Mittendorf, PhD

Bert Sweetman, PE, Phd

ABSTRACT

The effectiveness of numerical prediction of structural dynamic response is assessed for a wind mast support structure typical of wind turbines, but without the turbine itself. This effectiveness is assessed by comparison of predicted mechanical strain below the waterline of the structure with measured field data. Particular attention is paid to the effects of wave directional spreading. In the model, wave loads are generated from a series of simulated irregular time-histories associated a single significant wave height and period, but two distinct spreading parameters. Load predictions are based the Morrison equation and the structural response is computed by solving a finite element model of the structure in the time domain. Comparisons are based on the variances of the response process.

1. INTRODUCTION

Historically, design of offshore turbine structures has evolved from design of two well-known structural types: onshore turbines and offshore oil production platforms. Wave loading is a principal difference between onshore and offshore structures, and the techniques to predict these loads are based on existing methodologies proven to be effective for offshore oil platforms. However, offshore wind support platforms differ from oil platforms in several important ways: First, wind platforms generally have less area exposed to wave-loading and are considerably taller than oil platforms. This combination makes structural dynamics relatively more important because the natural frequency of the platform is often closer to frequencies at which there is meaningful wave energy. Second, wind farms often include large groups of platforms with very little variation between designs. Applying one design to multiple turbines, combined with the relatively slender profit margins in the offshore wind business, makes cost-optimization of the structural design important. Finally, wind turbines routinely reduce structural loading at times of maximum wind by operating at lower speed or shutting down the turbine completely.

This ongoing work is to quantify the effectiveness of wave load and response predictions through critical comparison between numerically predicted strain response and measured strain response on a wind-turbine support structure in the German Bight. Special emphasis is placed on quantifying the relative importance of including wave directional spreading as opposed to the more conventional unidirectional (long-crested) approach.

Forristall et al. (1978) observed considerable scatter between measured ocean wave velocities and predictions based on unidirectional theories (regular, irregular and also nonlinear) with a clear bias toward numerical overestimation of measured values. Gudmestad, O.T. (1998) confirms the importance of accurate water particle predictions for the calculation of dynamics and loads for offshore structures.

Current plans for offshore wind turbines are for shallow or intermediate water depths, where non-linear effects wave spreading may be important. In this paper the effect of spreading is explicitly included in the wave load calculation and its effects are quantified. Specifically, a directional sea state is simulated from a power spectrum combined with a directional spreading function and then used to predict wave loads and response of an offshore wind mast support structure. Finally, the results of this simulation and prediction are compared with full-scale measured field data from the Amrumbank wind mast structure. This work differs from the work of M. Hartnett and P. Mitchell (2000) in analysis of jacket platforms, because here the predictive capabilities and the relative importance of wave spreading are assessed in the time domain rather than applying a linearized frequency-domain approach.

2. DIRECTIONAL WAVE ENERGY DISTRIBUTION AND WAVE SIMULATION

In general, a power spectrum of a sea state, $S(f)$, expresses the distribution of wave energy as a function of wave frequency, f . Wave spectra are generally applied to long-crested seas, and have been effective for prediction of maximal loads because it is generally long-crested seas that result in these maxima. However, directionality may be more important for design of wind turbines because wind turbines are generally sited near shore, where directionality is more prevalent, and because wind turbines generally shut down in high winds, extreme loading conditions may actually occur in sea conditions other than the long-crested seas typical of extreme storms. Irregular waves specified by only a power spectrum appear as long-crested waves, which have straight and parallel crest-lines. The patterns observed under real conditions feature many component waves propagating in various directions. The concept of the directional spectrum has been introduced to describe a sea state containing directional components, or more specifically, to describe the directional distribution of wave energy [Pierson et al., 1955].

The commonly used cosine-2s model [Longuet-Higgins et al., 1963 and Mitsuyasu et al., 1975] is selected for this work to enable consistent comparison with the measured wave data, which was field-processed using the cosine-2s model. The spreading parameter, s , can be related to the directional width obtained from cross-spectral analysis of three signals collected by floating buoys: the buoy angle from vertical, the compass heading of that rotation, and the instantaneous water surface elevation (e.g., Cartwright, 1963). In that analysis, it is assumed that the instantaneous water surface elevation is made up of non-interacting waves and that the buoy follows the slope of the sea surface perfectly over the frequency range.

Mitsuyasu et al. (1975) published the following classification for the parameter s :

- $s=10$ wind wave
- $s=25$ swell generated nearby with short decay distance
- $s=75$ swell generated far away with long decay distance

Here, an irregular wave simulation is performed using a directional spectrum $F(f, \theta)$ parameterized by a JONSWAP spectrum in combination with a $\cos^2 s$ spreading function [Mitsuyasu et al., 1975]:

$$F(f, \theta) = S_{JONSWAP}(f) \cdot \frac{\Gamma(s+1)}{\pi^{0.5} \Gamma(s+0.5)} \cdot \cos^{2s}(\theta - \theta_0) \quad (6)$$

in which $S_{JONSWAP}$ is the JONSWAP wave power spectrum commonly used in the North Sea (Hasselmann *et al*, 1973), θ is the wave component direction, θ_0 is the main direction of the overall wave process, s is the spreading parameter and Γ is the gamma function.

A representation of an irregular realization of a water surface elevation $\eta(x,y,t)$ in space and time can be simulated from the directional spectrum as a superposition of a large number of elementary sine/cosine waves with random phase (e.g. Massel, 1996). The two sea-states used to generate the simulation results presented here both result from the directional JONSWAP with significant wave height $H_s=7.7\text{m}$, peak period $T_p=11.0\text{s}$, and differ only in the spreading parameter: $s=10$ or $s=75$. An analysis of the maximum crest velocities of every single zero-crossing wave indicates higher velocities (about 20%) in a unidirectional simulation than in the highly spread simulation ($s=10$) presented here.

3. WAVE LOAD SIMULATION

Here, wave loads are predicted for simulated sea states. The reduction of the particle kinematics within a directional wave simulation compared to the unidirectional approach directly reduces structural loads. The Amrumbank wind mast structure is a simple monopile with a diameter of 5 meters, a total height of 48 meters, located in a water depth of 30 meters. For this relatively small structure diameter, it is appropriate to use the Morison equation to estimate wave forces [Morison et al., 1950]. The resulting force acting on the structure due to non-breaking waves is composed of a summation of inertia and drag terms.

$$f \cdot dz = f_m + f_d = c_m \cdot \rho \cdot dV \cdot \frac{\partial u}{\partial t} + c_d \cdot \frac{\rho}{2} \cdot dA \cdot u \cdot |u| \quad (10)$$

in which c_m is the inertia coefficient, c_d the drag coefficient, ρ the fluid density, $dV = dx dy dz$ the differential volume of a structural element, $dA = dx dz$ the cross section and u the fluid particle velocity orthogonal to the cylinder axis.

Figure 1 summarizes the effect of changing the spreading parameter on total loads. Spreading parameter $s_1=10$ represents highly spread wind waves and $s_2=75$ represents swell conditions. The larger spreading (small parameter s) is associated with smaller loads than the less spread seas. Very small parameters s converge to long-crested (unidirectional) results.

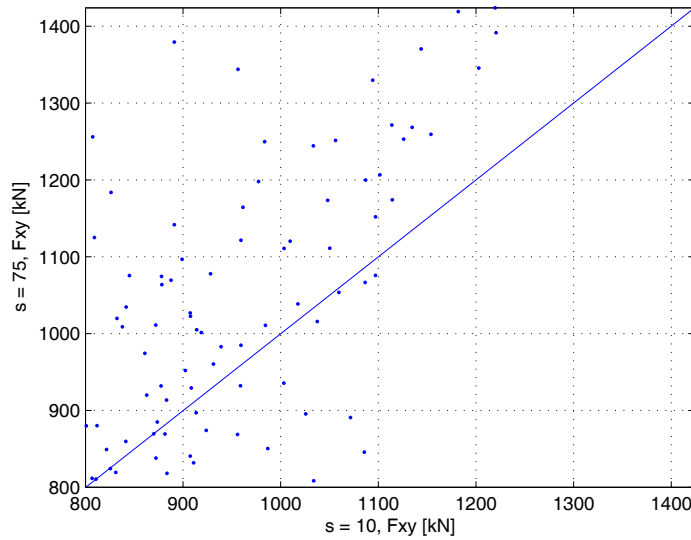


FIGURE 1— SCATTER PLOT OF TOTAL MORISON LOADS FOR VARYING SPREADING PARAMETERS.

4. ANALYSIS OF MEASURED DATA FROM THE AMRUMBANK MAST

The Amrumbank West measurement mast is a monopile structure located north-west of Helgoland Island (N 54°30' E 7°42') in 23 m water depth. Measured wave data are available for the period from November 2005 to September 2006 with 61% coverage. Significant wave heights, spectra, and spreading parameters, s , have been measured near the structure by a directional wave buoy for numerous 30-minute intervals. Unfortunately, only this summary data was recorded and not time-histories of the water-surface elevations.

Mechanical strain was measured below the waterline of the structure, and this measured strain data combined with the measured sea-states enables verification of the numerical load and response models applied here. Two pairs of strain gages are fixed to the structure at a vertical location in the water column. The strain is recorded by the four gauges, giving two orthogonal directions: north-west to south-east (NWSE), and south-west to north-east (SWNE). Each strain data set represents of a 30 minute time history recorded with a sample rate of 0.05Hz. The measured data covers November 2005 and January 2006. This strain data has been analyzed to determine its short-term statistical properties and has been observed to be reasonably stationary over each 30 minute interval. Results of the short-term analysis are used to investigate the distribution of the load and response energy over nautical direction.

4.1 DISTRIBUTION OF VARIANCE OF STRAIN ENERGY

The reaction stresses, as well as the internal forces and moments are directly determined from the measured, strain based on linear elastic material properties for steel (Haake et al.

in Zielke (Edt.), 2005). A time-history of the principal moment, M_H , is computed from the time-history of measured strains as:

$$M_H(t) = \varepsilon_{M,\psi}(t) \cdot E \cdot I / r \quad \text{in [kNm]}, \quad (11)$$

where E is the Young's modulus, $\varepsilon_{M,\psi}$ is principal strain, I is the cross-sectional moment of inertia and r is the radius of the cylinder. Time histories of the strain at specific physical locations on the cylindrical structure are computed as a function of direction by computing a principal strain magnitude and direction from the two measured strain components, then vectorially projecting that strain over several directional sectors ($\Delta=30^\circ$) covering all directions (0° - 360°). Specifically, the magnitude, $\varepsilon_{M,\psi}$ and direction, Ψ , of the principal strain, is determined from the two measured strain time histories as:

$$\varepsilon_{M,\psi} = -\frac{(\varepsilon_1 - \varepsilon_3) \cdot \cos(\psi) + (\varepsilon_2 - \varepsilon_4) \cdot \sin(\psi)}{2} \quad \text{in} \left[\frac{\mu\text{m}}{\text{m}} \right] \quad (13)$$

$$\psi = -\arctan\left(\frac{\varepsilon_1 - \varepsilon_3}{\varepsilon_2 - \varepsilon_4}\right) \pm 90 \quad \text{in} [^\circ]. \quad (14)$$

The resulting location-specific time histories are then transformed to power spectra. The variance of each resulting strain process is considered the strain energy and is plotted as a function of direction. Figure 2 shows good agreement between the direction of high wave energy and of high response energy.

The principal strain energy, regardless of direction on the structure, is plotted as a function of increasing spreading (Figure 3). The measured strain shows large variability. Linear regression (not shown) consistently shows the strain energy to slightly decrease with increased spreading.

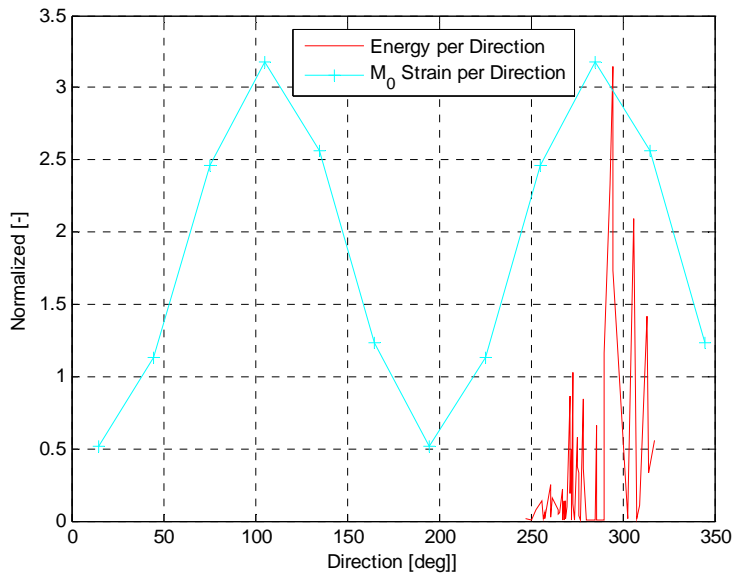


FIGURE 2 - STRAIN ENERGY AS A FUNCTION OF DIRECTION, MEASUREMENT FROM 2006-02-07-6:00 ($H_s=1.57$ m, $T_p=5.0$ s, $\theta_0=122^\circ$, $s=13$).

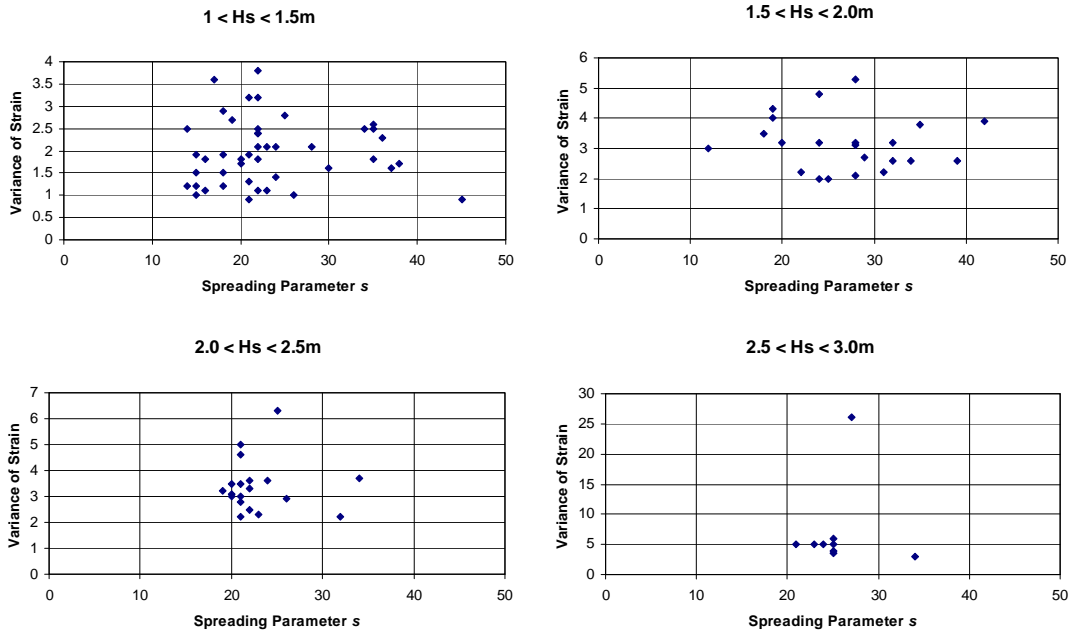


FIGURE 3 - PRINCIPAL STRAIN ENERGY (MICROMETERS/METER)² AS A FUNCTION OF SPREADING.

5. SIMULATION OF STRUCTURAL RESPONSE

A three dimensional finite element analysis of the wind measuring mast Amrumbank West has been performed to assess the effects of directional wave loads on the structure response. The finite element model used here was previously verified by Kossel (Kossel, 2006). The equations of motion are solved with a Newmark time integration scheme. Time-histories of the wave loads have been realized as outlined in Section 3, using algorithms previously verified by Mittendorf (2006).

Two numerical models of the structure were used in this analysis. One was extremely complicated, which included an explicit model of the wind mast. This complicated model was used to verify a more simplified finite element model accurately predicts the structural response. The simplified model represents the wind mast as a lumped mass near the end of a vertical member.

The sea state chosen for the simulation presented here is that which was measured on November 24th in 2005. It is characterized by a directional JONSWAP with significant wave height, H_s , of 3.08 m, peak period, T_p , of 7.14s, main propagation direction (θ_0) of 238° and degree of spreading, s , of 25. To obtain a meaningful distribution of the response, the simulation has been repeated one hundred times with different random phase vectors. Such a large number of simulations proved necessary because the random phases have been found to have a strong influence on the magnitude of the maximum and loads and response. Furthermore, the variance of the load process (total integrated horizontal forces, not shown) and strain response spectrum, M_0 , also show a large variability. This scatter of the response data is present in the measured data (Figure 3).

The variance of the time-histories of the principal strain of the simulated process is found to be reasonably well described by a log-normal distribution (Figure 4 and 5). All of the results shown on these plots results from the same sea_state (H_s , T_p , s); the very large range of response results entirely from changes to the irregular time-history associated with differing random phases.

Surprisingly, a scatter plot of the M_0 versus F_0 (6) shows almost no relationship between the applied environmental load and the associated strain response. This plot highlights the importance of considering structural dynamics in calculation of stress for either fatigue or maximum design load purposes. The load varies between 4500 kN and 10500 kN, whereas the strain varies between 2.5 $\mu\text{m}/\text{m}$ and 28 $\mu\text{m}/\text{m}$; to repeat, that substantial variation results exclusively from differences between the random phase vectors.

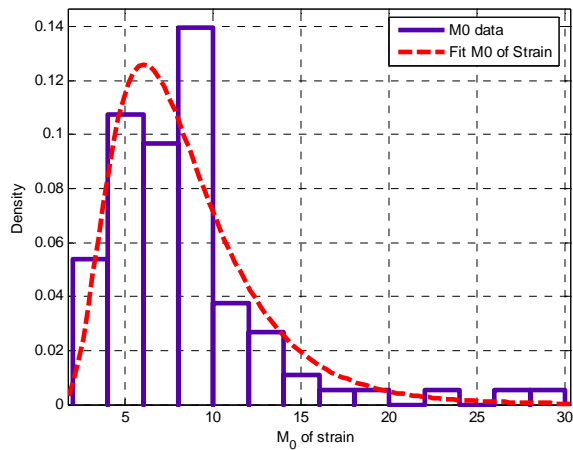


FIGURE 4 - LOG-NORMAL FIT OF THE STRAIN DATA.

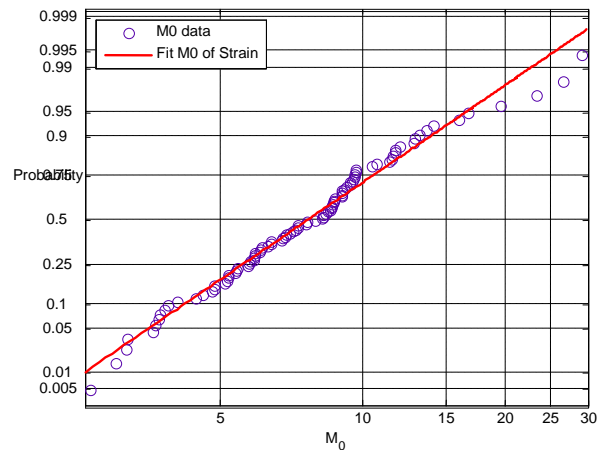


FIGURE 5 - LOG-NORMAL FIT OF STRAIN DATA. $\mu = 2.02039$ AND $\sigma = 0.468363$

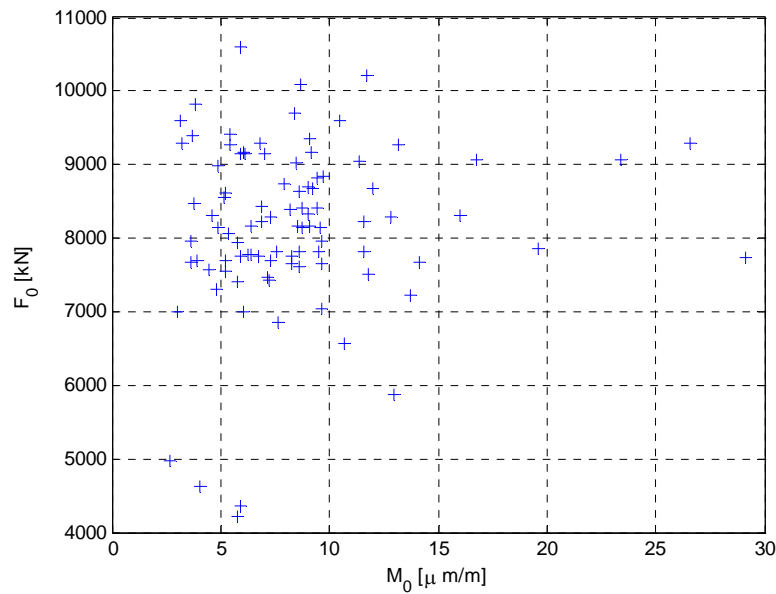


Figure 6 - Variance of load vs. variance of principal strain for simulated response data; $H_s = 3.08$ m, $T_p = 7.14$ s and $s=25$

6. CONCLUSIONS

The numerical model has been found to be in general agreement with the measured field data, though a detailed statistical analysis to quantitatively assess its effectiveness has not yet been completed because there is not yet enough measured data or simulated results for such an assessment to be meaningful. However, some interesting observations can be made from these preliminary results. First, the importance of wave spreading on both

loads and response is confirmed by Figure 1 for the loads and Figures 3 and 6 for the response: both show decreasing load or response with increasing spreading. This decrease is somewhat smaller than the authors had expected at the initiation of the study. Tremendous variability of the measured strain associated with a single sea-state was observed in the measured strain for both the measured (Figure 3) and simulated (Figures 4 and 5) data. This observation highlights the importance of application of statistical methods in the design of these structural types. The strain energy (variance of the process) of the simulated strain data for many realizations of a single sea-state appears to be well described by a log-normal distribution (Figures 4 and 5); unfortunately there is insufficient measured data for any one sea-state to confirm this observation. Finally, the surprisingly low correlation between simulated loads and simulated response shown in Figure 8 highlights the importance of considering the irregular response time-history in assessing mechanical strain due to structural dynamics.

7. ACKNOWLEDGMENTS

This work was supported by the Texas Institute of Oceanography and by the National Science Foundation, Division of Civil and Mechanical Systems under Agreement Number CMS-0448730. Any opinions, findings, and conclusions or recommendations expressed in this material are those of the authors and do not necessarily reflect the view of the National Science Foundation.

8. REFERENCES

Banner, M. (1989). Equilibrium spectra of wind waves. *Journal of Physical Oceanography*, 20:966 – 984.

Cartwright, D. E. 1963. The use of directional spectra in studying output of a wave recorder on a moving ship, *Ocean Wave Spectra: Proceedings of a Conference*, Prentice-Hall, Inc., 203-218, Inglewood Cliffs, NJ.

Goda, Y.: Numerical Experiments on Wave Statistics with Spectral Simulation. *Rep. of Port and Harbour Res. Inst.*, Vol. 9, No. 3, 1971.

Hasselmann, K., Barnett, T. P., Bouws, E., Carlson, H., Cartwright, D. E., Enke, K., Ewing, J. A., Gienapp, H., Hasselmann, D. E., Kruseman, P., Meerburg, A., Müller, P., Olbers, D. J., Richter, K., Sell, W., and Walden, H. (1973). Measurements of wind-wave growth and swell decay during the joint north sea wave project (JONSWAP). *Deutsche Hydrogr. Zeits. Reihe A*, 12.

Hudspeth, R., Asce, M. and Chen M.-C., Digital Simulation of Nonlinear Random Waves, *Journal of the Waterway Port Coastal and Ocean Division*, No. 14376, pp. 67 – 85, 1979.

Kossel, T., Wellenbelastungen auf die Tragstrukturen von Offshore-Konstruktionen“, Diploma thesis, Institute of Fluid Mechanics and Computer Applications in Civil Engineering Leibniz Universität Hannover, 2006.

Mitsuyasu, H., Tasai, F., Suhara, T., Mizuno, S., Ohkusu, M., Honda, T., and Rikiishi, K. (1975). Observations of the directional spectrum of ocean waves using a cloverleaf buoy. *Journal of Physical Oceanography*, 5:750 – 760.

Mittendorf, K., Hydromechanical Design Parameters and Design Loads for Offshore Wind Energy Converters, Dissertation, Univ. Hannover 2006

Morison, J.R., O'Brien, M.P., Johnson, J.W. and Schaaf S.A., The Force exerted by Surface Waves on Piles, *Pet. Trans., AIME*, 189, pp. 149 – 154, 1950.

Neumann, T., Nolopp, K., Strack, M., Herklotz, K., Stein, J. (2004): Assessment of one year of measurements on the first offshore wind research platform in the German Bight, FINO 1. DEWEK 2004.

Pierson, W. J., Neumann, G., and James, R.W. (1955). Practical methods for observing and forecasting ocean waves by means of wave spectra and statistics. U.S. Naval Office, 603.

Rychlik, I. (1987). A new definition of the rainflow cycle counting method. *Int. J. Fatigue*, 9:119 – 121.

Tucker, M. J. (2001). *Waves in Ocean Engineering*. Pergamon Pr., Textbook.

Wheeler, J. (1970). Method for calculating forces produced by irregular waves. *Journal of Petroleum Technology*, pages 359 – 367.

Zielke, W. (Editor), Haake, G., Böker, C., Richwien, W., Lesny, K., Hinz, P., Schaumann, P., Mittendorf, K., Haake, G., Annual Report GIGAWIND_{plus} 2005, <http://www.gigawind.de> (in German).

Gudmestad, O.T. (1998): On the importance of understanding ocean wave kinematics for calculations of dyn. and loads on offshore structures. *Int. OTRC Symposium: Wave '98*; pp. 1-8.

M. Hartnett and P. Mitchell (2000), An analysis of the effects of the leg-spacing on spectral response of offshore structures, *Advances in Engineering Software*, Volume 31, Issue 12, Pages 991-998.